PCCP

Accepted Manuscript

Journal Name

ARTICLE

Three Centered Hydrogen Bond of the type C=O…H(N)…X-C in diphenyloxamide derivatives involving halogens and a rotating CF$_3$ group: NMR, QTAIM, NCI and NBO Studies

A. Lakshmipriya[a,b], Sachin Rama Chaudhari[a,b], AbhishekShahi[c], E. Arunan[c], N. Suryaprakash[a,b,*]

The existence of three centered C=O…H(N)…X-C hydrogen bond (H-bond) involving organic fluorine, and other halogens in diphenyloxamide derivatives has been explored by NMR spectroscopy and quantum theoretical studies. The three centered H-bond with the participation of rotating CF$_3$ group and the F…H-N intramolecular hydrogen bonds, a rare observation of its kind in organofluorine compounds, has been detected. It is also unambiguously established by number of one and two dimensional NMR experiments, such as, temperature perturbation, solvent titration, ^{15}N-^{1}H HSQC, ^{19}F-^{1}H HOESY, and is also confirmed by theoretical calculations, such as, Quantum Theory of Atoms In Molecules (QTAIM), Natural Bond Orbital (NBO) and Non-Covalent Interaction (NCI).

Introduction

The bifurcated H-bonds are of two types, viz., a three centeredH-bond where a single hydrogen atom can participate in two different H-bonds, and the other is where two hydrogens get involved in H-bonds with same acceptor atom. An illustration of such type of interactions is given in scheme 1. Bifurcated H-bonds are generally observed in complex natural (or) synthetic organic molecules.[1] It is also well known that, in general, bifurcated H-bond is an essential step in water reorientation.[2] The three centered H-bonds occur more frequently in bio-macromolecules, such as, DNA.[3]Such type of weak interactions are also reported in the X-ray structure of an anti AIDS compound 3'-azido-3'-deoxythymidine (AZT)[4] and in synthetic molecules, such as, foldamers or oligomer architectures.[5] The specific H-bonding interactions found in bigger biomolecules have been modelled using small molecules.[6]In an earlier report the structure and conformation of oxamide derivatives have been established by NMR spectroscopy. The study convincingly established the trans geometry of these molecules due to the presence of bifurcated intramolecular hydrogen bond, where the two oxygen atoms is coordinated to a single hydrogen atom.[7]The present work is focused on the new class of halo derivatives of diphenyloxamide, molecules that are the basic units of foldamers, where the formation of three centered H-bond contributes to the stable and rigid structure. The possible mode of three-centered H-bond formation C=O…H(N)…X-C (where

X= CF$_3$, F, Cl, Br and I) in the diphenyloxamide derivatives is given in scheme 2. Although it is well established that organic fluorine hardly ever accepts H-bond[8–11], there are number of reported examples, where the organic fluorine is involved in intramolecular H-bond. The first and the rare observation of the engagement of CF$_3$group in N-H…F-C type H-bond in derivatives of benzanilide has recently been reported.[12]

In this work, number of one and two dimensional NMR experiments have been carried out to explore the existence of weak molecular interactions in all the investigated molecules. The observed experimental results have been corroborated with theoretical calculations, such as, Quantum Theory of Atoms In Molecules (QTAIM)[13], Natural Bond orbital (NBO)[14] and Non-covalent Interaction (NCI)[15].

Results and discussion

The chemical shift is one of the most widely employed NMR parameter to probe weak molecular interactions. Hence we have measured the concentration dependence variation of NH chemical shift (δ_{NH}) for all the molecules. It is observed that, δ_{NH} remained unaltered for all the molecules, irrespective of the concentration, giving ample evidence for the existence of intramolecular H-bond. The stack plot of ^{1}H-NMR spectra of investigated molecules recorded in the solvent CDCl$_3$ are reported in Fig.1.The aromatic region of the ^{1}H spectrum for molecule **1** reveals that the coupled proton spin system is of the type AA'BB'C and gives 3 groups of

Physical Chemistry Chemical Physics Accepted Manuscript

coupled multiplets with an intensity ratios of 2:2:1. This might be due to 180^0 aryl flips in this molecule. For molecules **2-6**, the aromatic protons are chemically in equivalent giving rise to four different groups of multiplets. This is another plausible proof for the rigid structure of these molecules. Assignment of protons can be carried out using chemical intuition and is reported in the supporting information. The chemical shifts of NH protons exhibit downfield shifts for the molecules, **2-6**, compared to the reference molecule **1**, indicating the participation of NH proton in additional weak molecular interactions, i.e, the possible H-bond in these molecules. The measured chemical shifts of NH protons in all the molecules and their differences with respect to molecule **1** are compiled in Table 1. It is evident from the Table 1 that there is a large variation in the NH chemical shift for the molecules, **2-6**, presumably due to the formation of a three centered H-bond. To unequivocally ascertain the existence of three centered H-bond, the molecules **7** and **8**, with the substitution of halogen group at the para position were also synthesized. Interestingly the large chemical shift difference was observed between the molecules **2** and **7** (0.23 ppm) and between the molecules **3** and **8** (0.6 ppm), which gave a strong evidence that the halogen group is participating in the three centered H-bond when the substituent is at the ortho position. This gives a logical evidence for the presence of three centered H-bond in the remaining three molecules. The proton acceptor trend for organic halogens in the intramolecular five membered ring of the type X…HO/HN follows Br >Cl> F.[16]This can also be inferred from the chemical shift difference between the molecules **2-5** and the molecule **1.**

Table 1: The chemical shifts of NH proton and their differences with respect to molecule **1**.

Molecule Number	Chemical shift (ppm) of NH proton in the solvent $CDCl_3$	Difference in chemical shift (ppm) with respect to molecule **1**
1	9.35	0.0
2	9.54	0.19
3	9.92	0.57
4	9.94	0.59
5	9.81	0.46
6	9.79	0.44
7	9.31	0.04
8	9.32	0.03

The lowering of temperature results in the strengthening of the H-bond and causes deshielding of proton. The deshielding of NH chemical shift on lowering the temperature is evident from Fig. 2A, and the values of calculated temperature coefficients ($\Delta\delta_{NH}/\Delta T$) are assimilated in Table 2. Larger value of temperature coefficient for molecule **1** compared to molecules **2-6** is a possible indication that

relatively the three centered H-bond is stronger than two centered one. However, in the present study, NH chemical shift changed drastically with respect to temperature. Usefulness of solvent titration in understanding such interactions is well known.[7,17]Therefore the solvent titration was carried out using DMSO-d_6. The DMSO-d_6 induced perturbation of δ_{NH} is reported in Fig. 2B and also the calculated values of $\Delta\delta_{NH}/\Delta V_{DMSO}$ are compiled in Table 2. The larger value of $\Delta\delta_{NH}/\Delta V_{DMSO}$ in molecule **1** compared to the molecules, **2-6**, is another indicator that three centered H-bond is relatively stronger than the two centered one.

Table 2: The calculated values of $\Delta\delta_{NH}$ as a function of temperature, as a function ofchange in the volume of DMSO-d_6, and the experimentally determined magnitudes of $^1J_{NH}$, for the molecules **1–6**. Please note that the couplings $^1J_{NH}$ and J_{NF} are negative due to negative gyromagnetic ratio of ^{15}N.

Molecule	$\Delta\delta_{NH}/\Delta T$ (Hz K^{-1})	$\Delta\delta_{NH}/\Delta V_{DMSO}$ (Hz μl^{-1})	$^1J_{NH}$ (Hz)
1	0.71	2.7	-91.3
2	0.65	0.98	-92.9
3	0.54	0.33	-92.0
4	0.58	0.37	-91.8
5	0.61	0.53	-90.8
6	0.26	0.43	-93.1

Another important NMR observable that provides direct evidence for the formation of H-bond is the coupling between the two NMR active nuclei involved in H-bond, where the spin polarization is transmitted through H-bond.[18–22] If the through space couplings are very small, many a times excessive broadening of NH signal due to ^{14}N quadruple relaxation prevents the precise measurement of such couplings, if any, that are hidden within the line width. In circumventing such problems, we have carried out 2D ^{15}N-^1H HSQC experiments for all the molecules, where ^{15}N is present in its natural abundance. The ^{15}N-^1H HSQC spectrum of molecule **6** in $CDCl_3$ yielded a quartet for the NH proton (reported in Fig. 3B) implying that the rotation of CF_3 group is very fast unlike the earlier report.[11] the^{15}N-^1H HSQC spectrum of molecule **2** in $CDCl_3$, reported in Fig.3A, yielded a doublet for the NH proton. However, the intriguing question remains to be answered is whether these couplings are covalent bond mediated or H-bond mediated. In seeking an answer to this question the ^{15}N-^1H HSQC experiments have been carried out in the H-bond disturbing solvent DMSO, where a singlet is detected for the molecule **6**, as reported in Fig. 4B. This unambiguously establishes the fact that there exists a three centered H-bond in the molecule **6**. But in DMSO solvent the molecule **2**yielded a doublet as reported in Fig. 4A, with the J_{HF}= 0.85 Hz and J_{NF} = -1.25 Hz, whereas in $CDCl_3$ these values are J_{HF} = 2.9 Hz and J_{NF} = -0.4 Hz respectively. The absolute value of J_{HF} is

larger in the solvent $CDCl_3$ compared to that in DMSO. Another interesting observation is that the relative slopes of the displacement vectors of the cross sections of the 2D HSQC experiments in the solvents (DMSO or $CDCl_3$) are opposite. This is indicated by the arrows in Figs. 2A and 3A. This implies that the relative signs of J_{HF} are also opposite in DMSO and $CDCl_3$. The techniques of determining the relative signs of scalar couplings using the slopes of the displacement vectors from different two dimensional NMR experiments is well known in the literature.[23–26] It may be mentioned that in the previous studies, the information on the relative signs of the couplings is derived by a single experiment. However, in the present study, interestingly this information is derived from ^{15}N-^1H HSQC experiments carried out in two different solvents. In the high polar solvent DMSO, which disrupts H-bond present in the system the measured couplings might be attributed to the covalent bond mediation only. On the other hand, in the case of nonpolar solvent $CDCl_3$, the measured J_{HF} value might be the contributions from both through space and through bond. From the values of J couplings obtained in both the solvents, the contributions from the hydrogen bond alone can be estimated. There are many reports on the signs and magnitudes of couplings involving hydrogen bond.[19,27–31] As reported earlier,[12,18,19] J_{HF} is negative, and hence its contribution is – 2.9 Hz (in $CDCl_3$) and +0.85 Hz (in DMSO). Then the contribution from the H-bond alone turns out to be -3.75 Hz. As far as signs of J_{NF} is concerned, it is known to be negative. These observations give a strong evidence for the presence of three centered H-bond in the molecule **2**.

To gain more insight, we have carried out 2D ^1H-^{19}F heteronuclear experiment (^1H-^{19}F HOESY)[32,33] which has been demonstrated to be powerful in identifying the presence of H-bond. The 2D ^1H-^{19}F HOESY spectra of molecules **2** and **6** are reported in Fig. 5. The observation of a cross-peak between ^1H and ^{19}F is an indicator of the involvement of fluorine in a weak molecular interaction.

The scalar coupling $^1J_{NH}$ has also been demonstrated to be a powerful tool in understanding the nature of H-bond. Thus for the purpose of deriving the $^1J_{NH}$, we have carried out the coupled ^{15}N-^1H HSQC experiments and the measured $^1J_{NH}$ values are reported in Table 2. Relative to molecule **1**, an increase in the $^1J_{NH}$ is observed in molecules, **2-4** and **6**, indicating the H-bond is predominantly an electrostatic in nature.[34–36] On the other hand, $^1J_{NH}$ decreasesinmolecule**5**, where the H-bond is mainly a covalent in nature.[20] There may be a possibility of formation of ci-isomers. However, this possibility is ruled out consequent to the established bifurcated nature of the hydrogen bonds in the investigated molecules.

The chemical shift of water peak was 1.54 ppm, which indicates probably there is no oxamide-water complex and the peak is due to water monomer[37]. To ascertain this the basic alumina was added to the solution. After adding alumina the chemical shift of water nearly remained constant. There could also be a possibility of dimerization, which could not be ascertained by the experiments carried out in the present study.

To ascertain the weak molecular interaction detected by NMR, the experimental results were compared with DFT calculations. All DFT calculations were carried out using G09

suite of program[38]. The B3LYP/6-311G** level of theory was used to optimize the structures of the molecules investigated. Considering various factors, such as, computational cost, reliability of the results and the presence of heavy atoms (e.g. I, Br, etc.) B3LYP/6-311G** level of theory was used for computation. To ensure that all optimized structures are global minima, harmonic vibrational frequency calculation was performed at the same level and all the real frequencies indicated that optimized geometry is minimum at potential energy surface. AIMAll[39] program was used for QTAIM calculations and Multiwfn[40] was used to plot NCI.

QTAIM calculations were carried out. In the present work, the magnitude of electron density (ρ) and sign Laplacian of electron density ($\nabla 2\rho$) are examined for H-bond determination. If the bond critical point (BCP) is present in between the two atoms, the bond paths joining the atoms through BCP indicates that both atoms are bonded. BCPs and bond paths for intramolecular H-bonds present in all the molecules are reported in Fig. 6. The values of electron density (ρ) and Laplacian of electron density ($\nabla^2\rho$) at each intramolecular BCPs are given in Table 3. These electron density values fall in the expected range (0.0102-0.0642 a.u.) for H-bonds.[41] The positive sign of Laplacian of electron density ($\nabla^2\rho$) at BCP indicates the type of interactions in all the molecule are hydrogen bonded. There is linear dependence of electron density with the binding energy and on this basis one can say that N-H…O H-bonds are stronger than the C-H…O H-bonds (Table 3). The proton acceptor trend for organic halogens in the intramolecular five membered N-H…X follows Br >Cl> I, as detected from the chemical shift difference between the molecules **2-5** with that of molecule **1**(*vide supra*). This trend is further supported by the ρ(NH…X) values (Table 3). It may be pointed out that in this study our aim is to give a qualitative idea about the H-bond energy by using the binding energy vs electron density correlation. Similar kind of approaches were used to calculate intramolecular hydrogen bond energy.[42] Moreover, a general equation [BE (kj/mol) = 777 x ρ (in a.u.) – 0.4, where BE is binding energy] is given to estimate the hydrogen bond energy from binding energy vs electron density correlation.[35] The electron densities values are about 0.015, 0.020 and 0.017 for NH...X, NH...O and CH...O, respectively (Table 3). Using the above simple equation, binding energies are estimated around 11, 15 and 13 kj for NH...X, NH...O and CH...O H-bond interactions, respectively. It is worth mentioning that above equation was proposed for inter-molecular bonding and also didn't account for the angular dependence.

For H-bond formation, electron transfer from the electron rich region of H-bond acceptor (in the present case lone pairs (lp) are the electron rich region) to the anti-bonding orbital (σ*) of the H-bond donor takes place. To study this property the Natural Bond Orbital (NBO) analysis have been carried out. The stabilization energy because of electron transfer for every H-bond is presented in the form of second order perturbation energy (E2) in each molecule and is given in the Table 4. The N-H…O bonds are stronger than the C-H…O bond, as seen by their E2 values.

Table 3: Electron density (ρ) and Laplacian of electron density ($\nabla^2\rho$) at BCP. $\rho(NH\ldots O)$ and $\nabla^2\rho(NH\ldots O)$ represent the electron density values and Laplacian of electron density values at the BCP which are present between NH and O-atom. The explanation of the remaining notations remains same. The calculations were done in both isolated and in the solvent chloroform. The values given in the parenthesis are the difference between isolated and solvent medium. It is very clearly evident that there is not much difference between them.

X	$\rho_{(NH\ldots X)}$	$\rho_{(NH\ldots O)}$	$\rho_{(CH\ldots O)}$	$\nabla^2\rho (NH\ldots X)$	$\nabla^2\rho (NH\ldots O)$	$\nabla^2\rho (CH\ldots O)$
H	--	0.0211(-0.0003)	0.0162	--	0.0924(-0.0008)	0.0575(0.0003)
F	--	0.0201	0.0160(-0.0002)	--	0.0922(-0.0005)	0.0567(0.0012)
Cl	0.0156	0.0205	0.0175(-0.0002)	0.0639	0.0925(-0.0004)	0.0635(0.0013)
Br	0.0159	0.0204	0.0179(-0.0003)	0.0561	0.0924(-0.0004)	0.0652(0.0015)
I	0.0154	0.0206	0.0185(-0.0003)	0.0454	0.0925(-0.0002)	0.0681(0.0018)
F(CF$_3$)	0.0138(0.001)	0.0211	0.0185(-0.0006)	0.0569(-0.0038)	0.0939(-0.0003)	0.0685(0.0031)

QTAIM calculations and NBO analysis could not show the intramolecular BCP for N-H…F interaction in molecule **2** which contradict the NMR observations. A newly developed and powerful method, NCI index was thus used to visualize the weak interaction which shows the presence of H-bond in molecule **2**, which is in agreement with NMR observation. In Fig. 7, the grid points are calculated and plotted for the two functions: sign(λ2)*ρ as function 1 and reduced density gradient (RDG) as function 2 by Multiwfn program. The function sign(λ2)*ρ is the multiplication of electron density with the sign of second Eigen value (λ2) of electron density Hessian matrix. RDG functions property is driven by gradient of electron density.[43] Both these functions contain the information about H-bonding and clubbing of these functions becomes a powerful method to probe H-bonding. Colour filled isosurface graphs have been plotted using these grid points by VMD program[42] (Fig. 8). For the molecules **3, 4**, and **5**, there are three spikes on the left hand side of the Fig. 7 which denote three H-bonds namely N-H…X, N-H…O and C-H…O (where X= Cl, Br, and I). These three bonds can be seen in the Fig. 8. Green and red coloured isosurfaces show weak H-bonds and steric effect. For X= F, all three bonds exist and the spikes corresponds to two H-bonds are overlapped (Fig. 7(2)). These 3 H-bonds are clearly seen by the presence of three isosurfaces in Fig. 8(2). For X = CF$_3$, this method shows four spikes, as can be seen in Figure 7(6). For equilibrium structure, the interactions between F-atoms and ortho H-atoms of both phenyl rings are revealed only by NCI plot. It may be pointed out that in NMR study, NH group appeared as a quartet due to fast rotation of CF$_3$ group. The observation of a quartet in ^{15}N-^{1}H-HSQC for the molecule **6** is mainly because of the free rotation of CF$_3$ internal rotor at ambient temperature. Relaxed potential energy scan for the H9-C5-C16- F2

dihedral angle was performed which established an internal rotation of CF$_3$ group (Fig. 9).The calculated barrier for this internal rotation is 2.15 kcal/mol using B3LYP/6-311G** level of theory. Typical energy barriers measured by NMR are 7-24 kcal/mol. That's why in NMR study, NH group appeared as a quartet due to the fast rotation of CF$_3$ group.

Table 4. The second order perturbation energy due to electron transfer (kcal/mol) for the intramolecular hydrogen bonds. The column heading gives the orbitals involved.

X=	lp(x) $\to$ σ*(N-H)	lp(O) $\to$ σ*(N-H)	lp(O) $\to$ σ*(C-H)
H	--	2.14	0.94
F	--	1.79	0.90
Cl	1.70	2.10	1.15
Br	2.43	2.15	1.21
I	2.60	2.67/0.55	1.77/0.70

Conclusions

The one and two dimensional NMR experiments revealed the existence of three centered H-bond in diphenyloxamide and its halo-derivatives, which is one of the rare observations and first of its kind. The presence of three centered H-bond observed experimentally in the molecules **3-6** is supported by the AIM and NBO analysis but not in the molecule **2**. On the other hand, its presence is established by 2D ^{15}N-^{1}H-HSQC spectra in two different solvents, and by the two-dimensional heteronuclear correlation experiment (HOESY). The new and powerful NCI calculations do confirm the presence of three centered H-bond in molecule **2** also. The solvents effects on coupling constants have an interesting application as far as the determination of relative signs of through-bond and through-space couplings in the molecule **2**is concerned. The three centered H-bond is found to be stronger than two centered H-bond which is unambiguously established by the temperature perturbation and DMSO solvent titration studies. It is also convincingly established that organic fluorine is a poor hydrogen bond acceptor in the formation of the intramolecular five-membered hydrogen bond of the type F…H-N.

Experimental Methods

NMR Measurements

All the investigated molecules **1-8** were synthesised following the procedure reported in ESI. The structure and the conformation of the molecule **1** has been reported earlier[7]. All the molecules were synthesised using the new procedure reported in ESI, and the presence of hydrogen bonding in them have been explored. The individual solutions of all the investigated molecules were prepared in the solvent $CDCl_3$.All the spectra were recorded using Bruker Avance 400 and 500MHz spectrometers. Temperatures were monitored by an Eurotherm variable temperature unit to an accuracy of $\pm 1.0^0$ C. The ^{1}H chemical shifts were referenced to tetramethylsilane. The nitromethane is used as an external reference. NMR titrations were carried out using a Bruker Avance 500MHzspectrometer. 2D ^{1}H-^{19}F HOESY[44] and ^{15}N-^{1}H HSQC[45] experiments were carried out using the well-known pulse sequence reported in the literature. Other experimental details are given in the supporting information.

Computational Methods

The presence of three centered H-bond in all the investigated molecules has been investigated using various theoretical studies like QTAIM, NBO and NCI. All DFT calculations were carried out using G09 suite of program. The B3LYP/6-311G** level of theory was used to optimize the structures of the molecules investigated. AIMAll program was used for QTAIM calculations and Multiwfn was used to plot NCI. Colour filled isosurface graphs have been plotted by VMD program. Relaxed potential energy scan for the H9-C5-C16-F2 dihedral angle was performed which established an internal rotation of CF_3 group.

Acknowledgements

Notes and references

[a] NMR Research Centre, Indian Institute of Science, Bangalore 560012, India. E:mail: nsp@sif.iisc.ernet.in, Tel: +918022933300, Fax: +918023601550

[b]Solid State and Structural Chemistry Unit, , Indian Institute of Science, Bangalore 560012, India.

[c]Inorganic and Physical Chemistry Department, Indian Institute of Science, Bangalore 560012, India.

Electronic Supplementary Information (ESI) available: [Procedure for synthesis of molecules and the ^{15}N-^{1}H HSQC Spectra of all the molecules].

1   M. Baron, S. Giorgi-Renault, J. Renault, P. Mailliet, D. Carré and J. Etienne, *Can. J. Chem.*, 1984, **62**, 526–530.

2   D. Laage and J. T. Hynes, *Science*, 2006, **311**, 832–835.

3   V. Fritsch and E. Westhof, *J. Am. Chem. Soc.*, 1991, **113**, 8271–8277.

4   U. Koch and P. L. A. Popelier, *J. Phys. Chem.*, 1995, **99**, 9747–9754.

5   J. Zhu, R. D. Parra, H. Zeng, E. Skrzypczak-Jankun, X. C. Zeng and B. Gong, *J. Am. Chem. Soc.*, 2000, **122**, 4219–4220.

6   C.-Y. Huang, L. A. Cabell and E. V Anslyn, *J. Am. Chem. Soc.*, 1994, **116**, 2778–2792.

7   F. J. Martinez-Martinez, A. Ariza-Castolo, H. Tlahuext, M. Tlahuextl and R. Contreras, *J. Chem. Soc. Perkin Trans. 2*, 1993, 1481–1485.

8   S. Alazet, K. Ollivier and T. Billard, *Beilstein J. Org. Chem.*, 2013, **9**, 2354–2357.

9   J. D. Dunitz and R. Taylor, *Chem. - A Eur. J.*, 1997, **3**, 89–98.

10   J. A. K. Howard, V. J. Hoy, D. O'Hagan and G. T. Smith, *Tetrahedron*, 1996, **52**, 12613–12622.

11   D. Chopra, *Cryst. Growth Des.*, 2012, **12**, 541–546.

12   S. R. Chaudhari, S. Mogurampelly and N. Suryaprakash, *J. Phys. Chem. B*, 2013, **117**, 1123–1129.

13   R. F. W. Bader, *R. F. W. Bader, Atoms in Molecules: A Quantum Theory, Oxford University Press, Oxford,* 1990.

Physical Chemistry Chemical Physics Accepted Manuscript

14 A. E. Reed, L. A. Curtiss and F. Weinhold, *Chem. Rev.*, 1988, **88**, 899–926.

15 J. Contreras-García, W. Yang and E. R. Johnson, *J. Phys. Chem. A*, 2011, **115**, 12983–12990.

16 R. a. Cormanich, M. P. Freitas, C. F. Tormena and R. Rittner, *RSC Adv.*, 2012, **2**, 4169–4174.

17 S. H. Gellman, G. P. Dado, G. B. Liang and B. R. Adams, *J. Am. Chem. Soc.*, 1991, **113**, 1164–1173.

18 G. N. Manjunatha Reddy, M. V Vasantha Kumar, T. N. Guru Row and N. Suryaprakash, *Phys. Chem. Chem. Phys.*, 2010, **12**, 13232–13237.

19 Divya Kumari , H.Sankeerth and N. Suryaprakash, *Chem. Phys. Lett.*, 2012, **525-526**, 129–133.

20 A. J. Dingley, J. E. Masse, R. D. Peterson, M. Barfield, J. Feigon and S. Grzesiek, *J. Am. Chem. Soc.*, 1999, **121**, 6019–6027.

21 A. Dunger, H. Limbach and K. Weisz, *J. Am. Chem. Soc.*, 2000, **122**, 10109–10114.

22 T. Axenrod, P. S. Pregosin, M. J. Wieder, E. D. Becker, R. B. Bradley and G. W. A. Milne, *J. Am. Chem. Soc.*, 1971, **93**, 6536–6541.

23 B. Baishya and N. Suryaprakash, *J. Chem. Phys.*, 2007, **127**, 214510.

24 B. Baishya, U. R. Prabhu and N. Suryaprakash, *J. Magn. Reson.*, 2008, **192**, 101–111.

25 B. Baishya, G. N. M. Reddy, U. R. Prabhu, T. N. G. Row and N. Suryaprakash, *J. Phys. Chem. A*, 2008, **112**, 10526–10532.

26 Lokesh,S. R. Chaudhari and N. Suryaprakash, *Chem. Phys. Lett.*, 2014, **602**, 40–44.

27 N. S. Golubev, I. G. Shenderovich, S. N. Smirnov, G. S. Denisov and H.-H. Limbach, *Chem. - A Eur. J.*, 1999, **5**, 492–497.

28 H. Benedict, I. G. Shenderovich, O. L. Malkina, V. G. Malkin, G. S. Denisov, N. S. Golubev and H. Limbach, *J. Am. Chem. Soc.*, 2000, **122**, 1979–1988.

29 I. G. Shenderovich, P. M. Tolstoy, N. S. Golubev, S. N. Smirnov, G. S. Denisov and H. Limbach, *J. Am. Chem. Soc.*, 2003, **125**, 11710–11720.

30 I. Alkorta, J. Elguero, R. M. Claramunt, C. López and D. Sanz, *Heterocycl. Commun.*, 2010, **16**, 261–268.

31 I. Alkorta, J. Elguero, H.-H. Limbach, I. G. Shenderovich and T. Winkler, *Magn. Reson. Chem.*, 2009, **47**, 585–592.

32 P. S. Pregosin, P. G. A. Kumar and I. Fernández, *Chem. Rev.*, 2005, **105**, 2977–2998.

33 A. Bagno, F. Rastrelli and G. Saielli, *Prog. Nucl. Magn. Reson. Spectrosc.*, 2005, **47**, 41–93.

34 A. V Afonin, I. A. Ushakov, L. N. Sobenina, Z. V Stepanova, O. V Petrova and B. A. Trofimov, *Magn. Reson. Chem.*, 2006, **44**, 59–65.

35 M. M. King, H. J. C. Yeh and G. O. Dudek, *Org. Magn. Reson.*, 1976, **8**, 208–212.

36 C. Vizioli, M. C. Ruiz de Azua, C. G. Giribet, R. H. Contreras, L. Turi, J. J. Dannenberg, I. D. Rae, J. A. Weigold and M. Malagoli, *J. Phys. Chem.*, 1994, **98**, 8858–8861.

37 M. Nakahara and C. Wakai, *Chem. Lett*, 1992, **21**, 809–812.

38 G09 Reference see ESI for details, .

39 *AIMAll (Version 13.11.04), Todd A. Keith, TK Gristmill Software, Overl. Park KS, USA, 2013*.

40 T. Lu and F. Chen, *J. Comput. Chem.*, 2012, **33**, 580–592.

41 A. Shahi and E. Arunan, *Phys. Chem. Chem. Phys.*, 2014, **16**, 22935–22952.

42 W. Humphrey, A. Dalke and K. Schulten, *J. Mol. Graph.*, 1996, **14**, 33–38.

43 E. R. Johnson, S. Keinan, P. Mori-Sánchez, J. Contreras-García, A. J. Cohen and W. Yang, *J. Am. Chem. Soc.*, 2010, **132**, 6498–6506.

44 J. Battiste and R. Newmark, *Prog. Nucl. Magn. Reson. Spectrosc.*, 2006, **48**, 1–23.

45 G. Bodenhausen and D. J. Ruben, *Chem. Phys. Lett.*, 1980, **69**, 185–189.
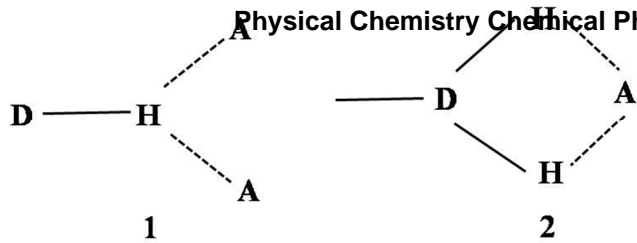
Scheme 1: The illustration of two different types of bifurcated H-bonds.
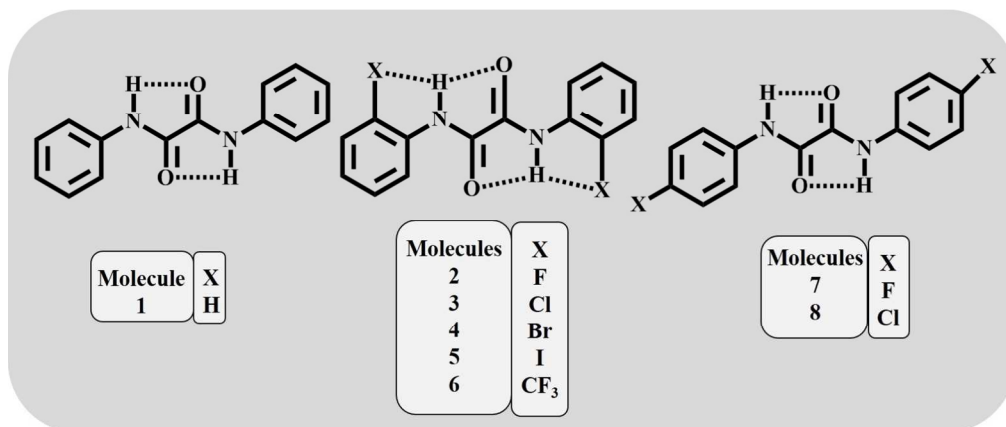
Scheme 2: Chemical structures of N,N-Diphenyloxamide (**1**) and its derivatives (**2-8**). The dotted line indicates the H-bond.
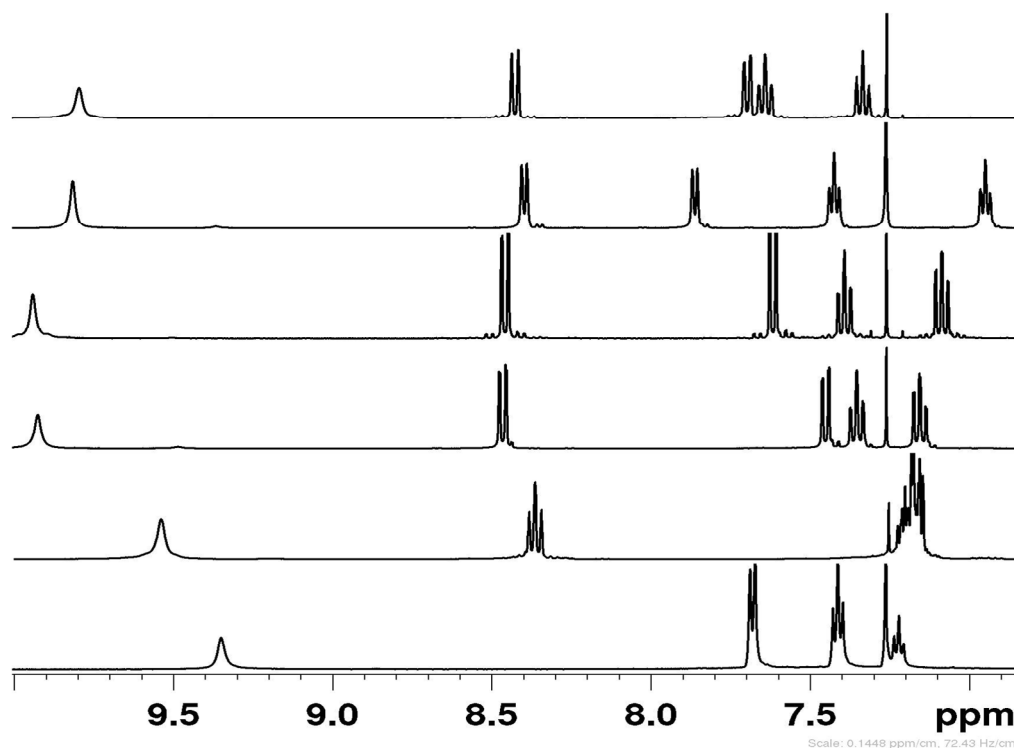

Figure1: Selected regions of the 400 MHz ^{1}H-NMR spectra of molecules **1-6** (from bottom trace to top trace), recorded in the solvent CDCl$_3$ at temperature 298 K and the spectra were referenced to internal tetramethylsilane.
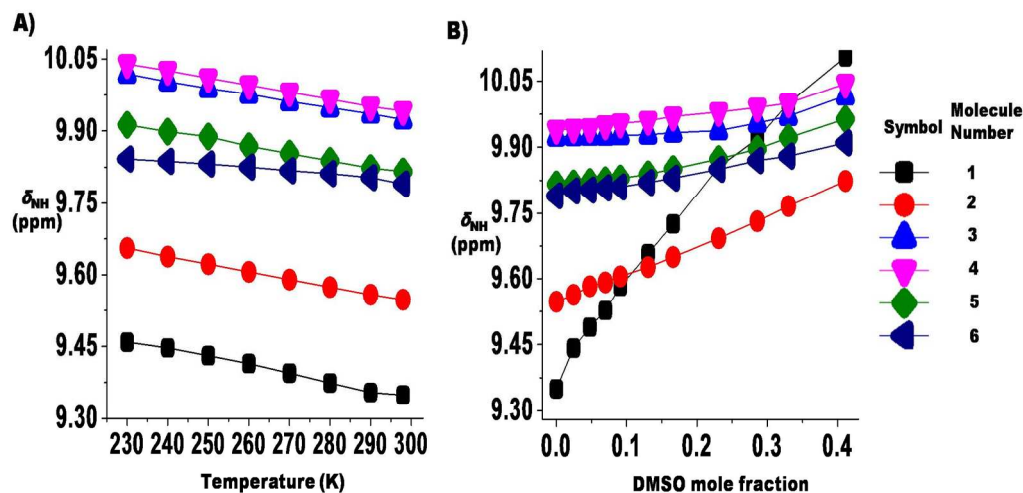
Figure 2: (A) The variation of the chemical shift of NH proton with temperature for the molecules, **1-6,** in the solvent CDCl$_3$ (10 mM concentration); (B) The variation of the chemical shift of NH proton with the incremental addition of DMSO-d$_6$ to the solution containing 200 µl of CDCl$_3$ (10 mM concentration) at 298 K for the molecules, **1-6**.
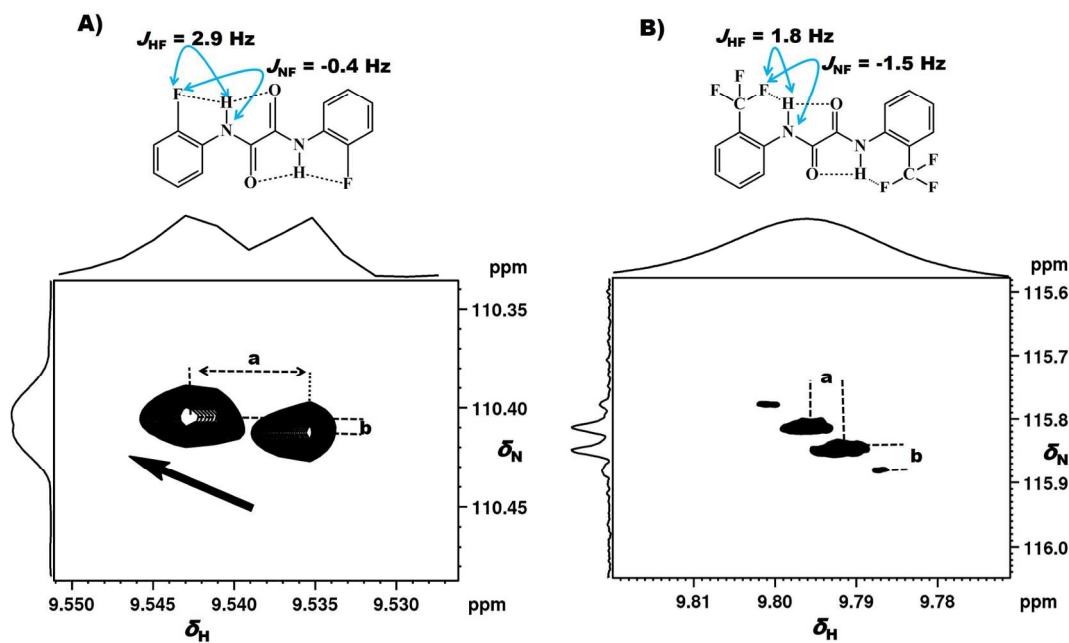
Figure 3: A and B) ^{1}H decoupled ^{15}N-^{1}H-HSQC spectra of the molecules **2** and **6** respectively, in the solvent CDCl$_3$. The molecular structures and the measured couplings have also been reported.

a) J_{HF} = 0.85 Hz
b) J_{NF} = -1.25 Hz
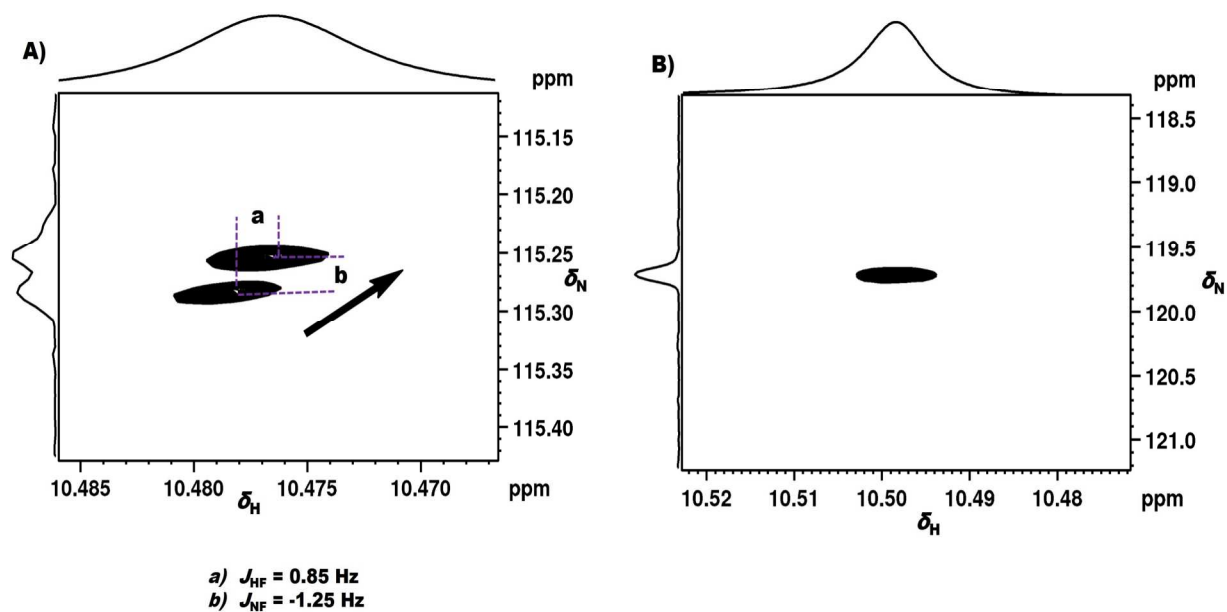
Figure 4: A and B) ^{1}H decoupled ^{15}N-^{1}H HSQC spectra of the molecules **2** and **6** respectively, in the solvent DMSO.
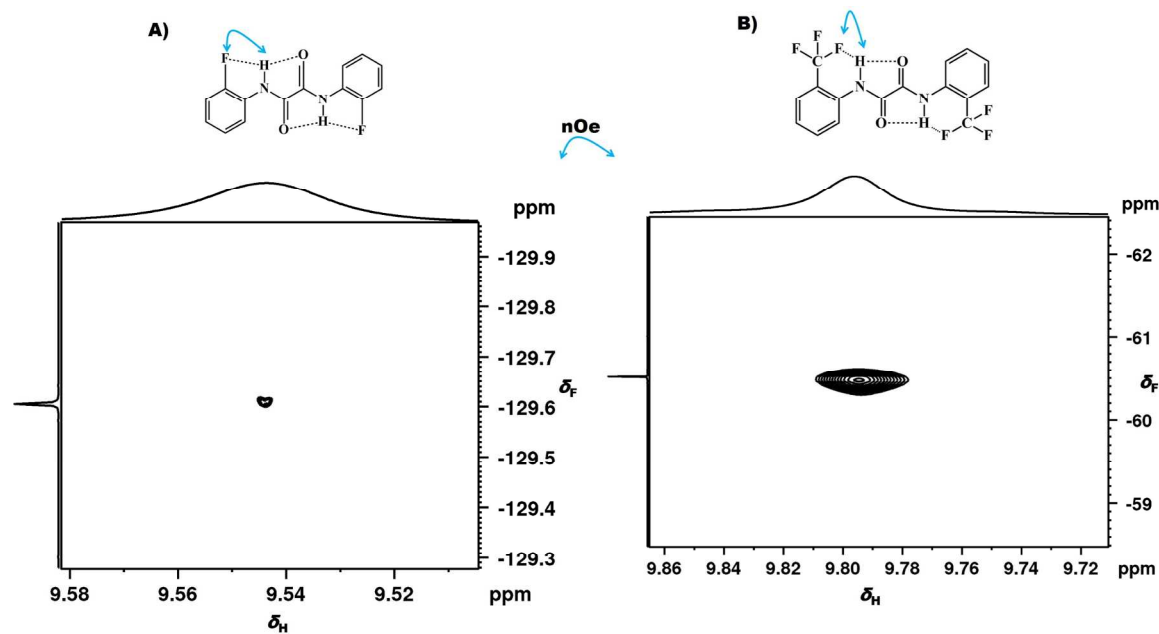

Figure 5: Two dimensional [1]H-^{19}F HOESY spectra of the molecules; A) **2** and B) **6**. The correlation between NH proton with CF_3 is evident from the detection of a strong cross peak. The mixing time used in the experiment is 450 ms.
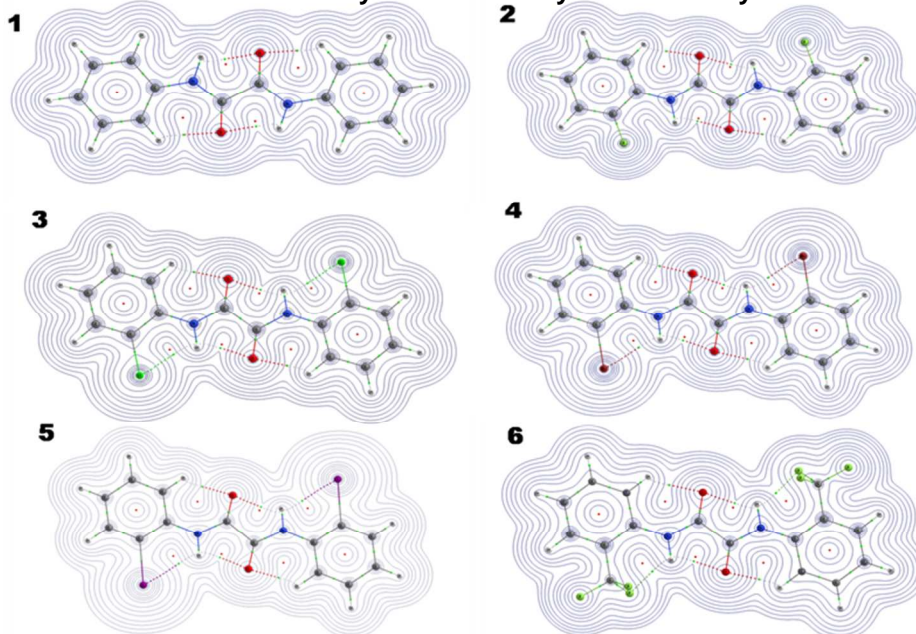
Figure 6: Molecular graphs, contour plots and AIM calculated bond paths for the molecules **1-6**. Dotted lines indicate the intramolecular H-bonds. Green and red dots are bond critical points (BCP) and ring critical points (RCP), respectively. Electron density is plotted as contours in the blue curves in the plane of molecules.
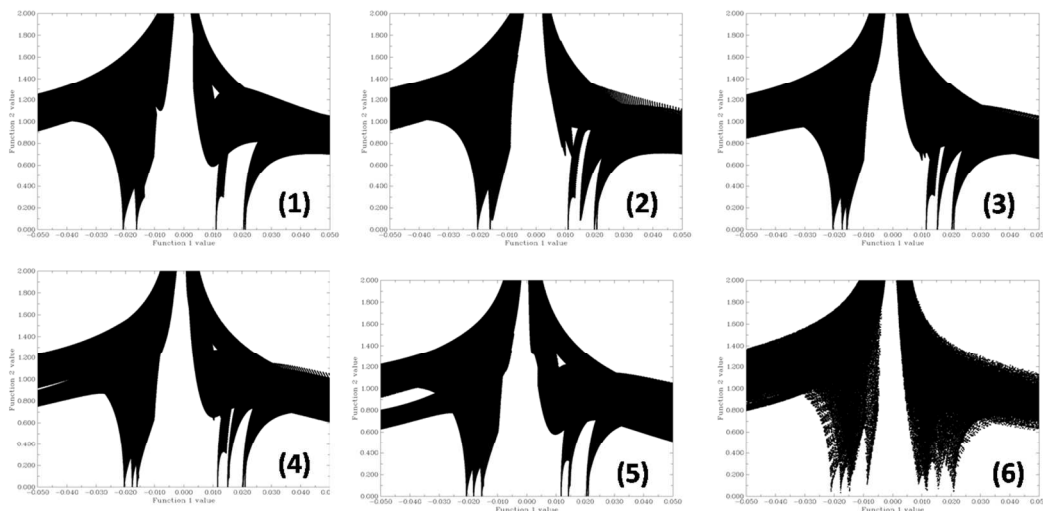

Figure 7.The plot of function 1 (sign(λ2)*ρ values) on X-axisvs function 2, the reduced density gradient (RDG) on Y-axis. Labels 1-6 represent molecules **1-6**, respectively.
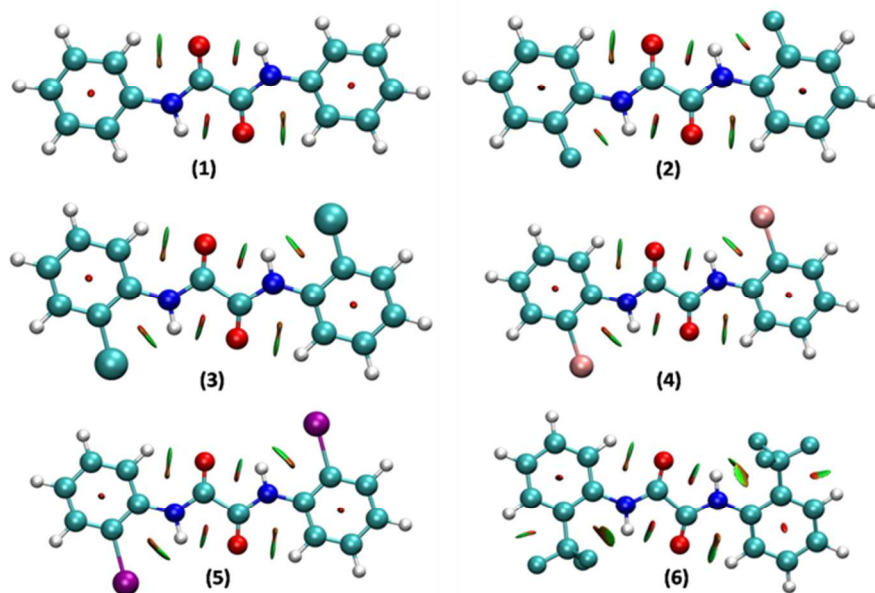
Figure 8. Labels 1-6 represent molecules **1-6**, respectively. Green colorisosurface denotes weak H-bond and red color stands for steric effect.
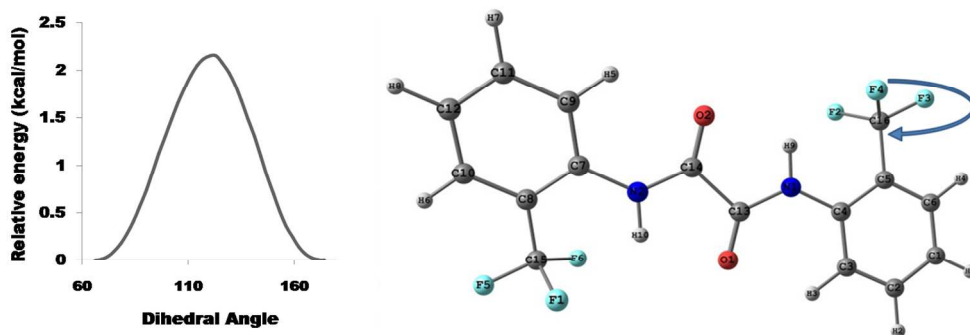

Figure 9: Relaxed potential energy surface for the internal rotation of CF_3 group at B3LYP/6-311G** level of calculation. The dihedral angle H9-C5-C16-F2 has been selected for the scan.

Physical Chemistry Chemical Physics Accepted Manuscript

Graphical abstract: